Wet Air Oxidation of Acetovanillone over LaFeO3 as Catalyst: A Model Reaction for Lignin Valorization

Wet Air Oxidation of Acetovanillone over $LaFeO_3$ as Catalyst: A Model Reaction for Lignin Valorization

Simone Ansaloni, Nunzio Russo and Raffaele Pirone*

Department of Applied Science and Technology (DISAT), Politecnico di Torino, Corso Duca degli Abruzzi, 24, 10129 Torino, Italy

Abstract: Wet air oxidation (WAO) of lignocellulosic biomasses is a promising route for the production of renewable and valuable compounds. In this work, acetovanillone (AV) was selected as lignin model molecule in order to investigate its behavior under the WAO reaction conditions. The experiments were carried out in a pressurized 50 ml batch reactor loaded with NaOH 2M as solvent, the reaction takes 1 h with temperatures ranging from 130 to 190 °C and air pressures between 5 and 30 bar. The perovskite-type mixed oxide $LaFeO_3$ was synthetized and used as heterogeneous catalyst in order to improve the activation of molecular oxygen. Vanillin yield resulted to benefit from high reaction temperature showing a maximum carbon yield of 22%, instead the formation of carboxylic acids from the oxidative degradation of AV largely benefits from high pressure of air, exhibiting an overall carbon yield of 35%. The produced compounds include oxalic, glycolic, lactic, malonic, and levulinic acid.

Keywords: Acetovanillone, Vanillin, Lignin, Carboxylic acids, Perovskite oxides, Wet air oxidation.

1. INTRODUCTION

The global demand of petrol-based derivatives continues to grow as the world population increases. In this regard, the development of an efficient model of integrated biorefinery based on renewable biomasses seems to be fundamental to ensure a sustainable production of fuels and chemicals [1]. However, despite years of research the creation of a commercial plant for biomass-to-biofuel conversion is still economically tricky [2]. In this sense, the association of fuels production with highly valuable chemicals one, may offer the opportunity to achieve the economic sustainability necessary to challenge the well-established oil-based industry [3]. As example, the production of bioethanol from sugars represents a settled process that, in the future, will be probably coupled with the production of sugars-derived building blocks for the chemical industry such as 5-hydroxymethylfurfural, polyalcohols and carboxylic acids (CAs) [4-6].

The lignin fraction of biomasses is an underexploited resource due to its recalcitrant structure, despite it represents an incredible origin of renewable chemicals [7, 8]. In fact, lignin is mostly considered as a byproduct waste of the cellulosic transformation, and it is generally burned to provide energy [9,10]. The wet air oxidation (WAO) of lignin offers an great opportunity for the production of renewable chemicals, in particular functionalized aromatics and dicarboxylic acids (DCAs) [2, 11-13]. The WAO involves the use of pressurized air as primary oxidant for the cleavage of the lignin matrix in an aqueous media, with relatively mild reaction temperatures and short reaction times [14].

Several classes of catalysts were studied in order to boost the performances of the WAO of lignin (CWAO), homogeneous metal ions [15], noble metals-based catalyst [14], and transition metals-based catalysts [16]. Perovskite-type oxides seems to be one of the most promising family of materials for the CWAO of lignin, due to their high oxidative activity, robustness and relative affordability [17-19]. However, the variability of the origin of the lignin, used as substrate in the previous studies in literature, generates great difficulties to achieve general conclusions on the performances of the processes, and more efforts are needed in order to clarify the reaction behavior.

Herein, we investigate the reaction behavior of acetovanillone (AV) as a model molecule for lignin during an analogue WAO process. Little work has been done so far in order to understand the oxidation behavior of lignin acetoderivates, and to enlighten the mechanisms which led to their degradation to low molecular weight CAs [20]. WAO tests carried out with model molecules may facilitate the comparison of the performances of different lignin valorization approaches, rather than compare the results obtained by using lignin with unclear origins and characteristics.

One of the main products obtained from the direct oxidation of AV, but also from lignin, is vanillin, a

*Address correspondence to this author at the Department of Applied Science and Technology (DISAT), Politecnico di Torino, Corso Duca degli Abruzzi, 24, 10129 Torino, Italy; Tel: +39 011 0904735: Fax: +39.011.090.4624;
E-mail: raffaele.pirone@polito.it

E-ISSN: 2408-9834/16

molecule considered as a commodity for its importance in the food and cosmetics industry [21-23]. Vanillin represents also an attractive aromatic molecule bearing diversified functional groups (hydroxy, methoxy and aldehyde) which can be exploited to synthetized various chemicals or bio-based polymers [24-26].

Moreover, many studies reported the formation of CAs from lignin oxidation, however, only few provide a characterization of the generated products without always highlight the potential of this renewable source of building blocks [27]. In particular, it was claimed the possibility to achieve the 50%$_{wt}$ of CAs from the alkaline oxidation of hardwood lignin with H_2O_2, giving mainly oxalic, formic, acetic, malonic, and succinic acid [28]. Furthermore, it was reported that different lignin model molecules can be oxidized to DCAs through quinone intermediates by using hydrogen peroxide at 60 °C over a chalcopyrite catalyst [29]. Concerning the WAO of lignin and lignin fractions towards CAs only limited work is present [30]. In this regard, the investigation has paid particular attention to products characterization, in order to evaluate the effect of the process parameters on the generated compounds, and to identify which factors mainly drive the evolution of the WAO of AV. Lastly, a perovskite-type oxide, namely $LaFeO_3$, prepared through the solution combustion synthesis technique (SCS), is introduced as catalyst in order to boost the oxidative properties of the system.

2. EXPERIMENTAL

2.1. Materials

All metal salts, organic molecules and solvents were purchased from Sigma Aldrich, and used as received. All gas cylinders were supplied by SIAD S.p.A., Bergamo (Italy).

2.2. Catalyst Preparation and Characterization

The $LaFeO_3$ tested in this study was prepared with the solution combustion synthesis (SCS) technique which involves the dissolution of $La(NO_3)_3 \cdot 6H_2O$ (2.16 g) and $Fe(NO_3)_3 \cdot 9H_2O$ (2.02 g) as metals source in 15 ml of water (0.33 M La and 0.33 M Fe) followed by mixing with the combustible, in this case 20 ml of urea solution (1.75 M) in a molar ratio 1:7 La over urea. Afterwards, the crucible with the 35 ml of reagents mixture was put in an oven at the ignition temperature of 600 °C, where the reaction readily starts and the crucible reaches temperature higher than 1000 °C allowing the formation of metal oxide powders [17, 31].

The Brunauer-Emmett-Teller (BET) specific surface area and pores properties were measured by nitrogen adsorbtion-desorbtion isotherms obtained in liquid nitrogen at 77 °K with Micrometrics Tristar II 3020 apparatus. The catalysts were previously degassed at 150 °C under nitrogen flow for 3 h by means of a Micromeritics Flow Prep 060 degassing system.

The reductive properties were studies with the temperature programmed reduction (TPR) technique by means of a Thermoscientific TPD/R/O 1100 analyzer equipped with a thermal conductivity detector (TCD). A fixed catalyst bed was enclosed in a quartz tube and sandwiched between two quartz wool layers, following, the samples undergone a pretreatment step at 120 °C (heating rate 20 °C/min, hold for 30 min) to remove residual water and contaminants under argon flow. After cooling, the sample was heated from room temperature to 850 °C (heating rate 5 °C/min) under a 20 ml/min hydrogen flow (5% in argon), the desorbed is detected by means of the TCD detector.

The morphology of these materials was studied by means of a Field Emission Scanning Electron Microscopy (FESEM) instrument, model Zeiss Merlin microscope, equipped with a GEMINI II column and an EDS detector.

The X-ray diffraction (XRD) patterns were collected with a Panalytical X'Pert Pro diffractometer using a CuKα radiation in the range 2θ=10÷90 with 0.01 step and 240 s of time per step. JCPDS files were used as reference to identify the present phases.

X-ray photoelectron spectroscopy (XPS) was carried out by means of a PHI 5000 Versa Probe (USA), equipped with a scanning ESCA microscope fitted with an Al monochromatic X-ray source (1486.6 eV, 25.6 W) and beam diameter of 100 μm. Curve-fits were performed with CasaXPS software (version 2.3.16).

2.3. WAO Reactions and Parameters Control

The catalytic tests were carried out in a stainless steel 50 ml stirred batch reactor 4590 provided by Parr Instruments Co. (USA), equipped with a pressure transducer, temperature and mixing speed controller. In standard conditions the reactor was loaded with 25 ml of NaOH aqueous solution 2 M and 3.5 g/l of AV, when used, the catalyst concentration was 0.4 g/l. The reactor head space was filled with pressurized air before turning on the heating system, the stirrer which was set at the speed of 800 rpm with a PBT-type

propeller, it worth noting that the heating ramp took 10 to 25 min. At the end, the reactor was cooled with cold water until room temperature, the gas phase was analyzed with an at-line gas chromatograph while the reaction mixture was filtered over nylon septa to recover the catalyst, neutralized with HCl, and extracted with ethylacetate (EtOAc) in order to recover the aromatic products.

2.4. Products Analysis

The EtOAc phase was dehydrated with $MgSO_4$ before being analyzed by means of a gas chromatograph (Agilent 7890A) equipped with a mass spectrometer (Agilent 5975B) and a proper capillary column (Agilent DB-5ms). The calibrations standards for the quantitated products were prepared in EtOAc as well. Decane was used as internal standard for the quantitation.

The aqueous phase was analyzed with a Shimadzu HPLC instrument equipped with a Phenomenex Rezex ROA organic acids H^+ column (300 x 7.8 mm) operating at 60 °C and eluent flow of 0.6 ml/min. Initially, the composition of the mobile phase is 5 mM H_2SO_4 in water which is progressively added of acetonitrile up to 15% in 10 min, following, the concentration newly decreases to return to the initial conditions in 60 min of total analysis cycle. The products were determined by means of a Photodiode Array Detector (PDA) set at 212 nm and internal calibration with propionic acid as standard.

The products present in the aqueous fraction were occasionally qualitatively analyzed with a GC-MS, for this purpose the samples were previously dried at 50 °C under vacuum, the organic compounds were dissolved in tetrahydrofuran (THF), added with the silylating agent BSTFA-TMCS 99:1 (N,O-bis (trimethylsilyl) trifluoroacetamide) - (trimethylchloro-silane), and left stirring overnight.

The AV conversion and the yield of vanillin contained in the EtOAc were calculated on molar base according with the reaction if Figure **1**. Alternatively, the yields were calculated by means of equation (1) on the base of the carbon content (Y $\%_c$) by taking into account the moles of the single compound (n_i), the number of carbon atoms in the molecule (N_i), and similarly, moles (n_{van}) and number of carbon atoms of the initial vanillin (N_{van}). The distribution of the products in the aqueous phase was calculated on molar base abundance.

$$Y\ \%_c = \frac{\sum (n_i \times N_i \times MW_C)}{(n_{van} \times N_{van})} \times 100 \quad (1)$$

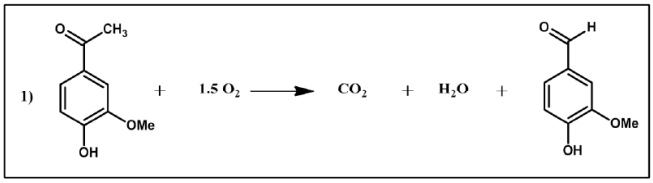

Figure 1: Stoichiometric oxidation of acetovanillone to vanillin.

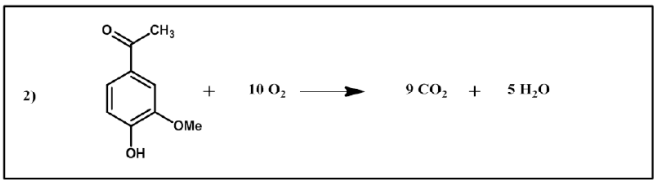

Figure 2: Total oxidation of acetovanillone.

3. RESULTS AND DISCUSSION

3.1. Wet Air Oxidation of Acetovanillone

In order to elucidate the reaction behavior of lignin fragments during a WAO process and to understand which reaction parameters mainly influence the performances, we introduced acetovanillone (AV) as substrate and model molecule. The adopted process set-up, reaction downstream procedures and products analysis, was the same in all tests as reported above, which follows a comparable methodology as the one used in previous similar studies on lignin oxidation [29]. The choice of $NaOH_{aq}$ 2M as solvent is due to the need of simulating a realistic WAO process involving lignin which is more likely to dissolve in alkaline media [32].

The only compound obtained in relevant amount in the extracted organic phase was vanillin, generated from the oxidation of the ketone group of AV, the reaction has a stoichiometric oxygen demand of 1.5 moles per mole of AV as shown in equation 1, corresponding to 3.7 bar of air in the adopted reaction setup. Other molecules typically observed in similar processes, such as vanillic acid, guaiacol, 3-hydroxyacetophenone and phenol, were occasionally observed in traces amount. Vanillin constitute also the first oxidation step of AV, further oxidative reaction lead to the generation of carboxylic acids and carbon oxides, the maximum oxygen request is obviously represented by the total combustion of AV to CO_2 which needs 10 moles of O_2 per mole of AV as shown in Figure **2**. Furthermore, it was reported that during the oxidation of lignin model molecules in alkaline media,

heavy weighted biphenyl structures can be occasionally formed [33, 34]. Unfortunately, these compounds resulted to be recalcitrant to further oxidative degradation, and may cause an increase in the amount of carbon lost from the products quantitation. Differently, the residual aqueous phase presents several types of CAs derived from the oxidative degradation of AV, these were identified by means of GC-MS as oxalic, glycolic, malonic, lactic and levulinic acid. Despite that, the imperfection of the silylating technique suggests the use of HPLC for the quantification of the compounds in the aqueous phase, however, the resolution achieved with this instrument was lower than what was achieved with the GC-MS, limiting the quantitation to the main compounds.

3.2. $LaFeO_3$ Characterization

The nitrogen desorption analysis (BET) of the prepared $LaFeO_3$ exhibited a total surface area of 12.1 m^2/g, with a BJH-pore volume of 0.049 cm^3/g, and average BJH-pore size of 180 Å. These values are in agreement with the BET results generally observed in materials prepared through SCS [35].

The X-ray diffraction pattern of the prepared catalyst is shown in Figure **3**, and it largely matches with the reference spectra of $LaFeO_3$ with orthorhombic crystal structure reported in the JCPDS reference database (00-037-1493). Exceptions are represented by the peaks at 32.5° and 44.5°, the first one belongs to La_2O_3 impurities with hexagonal structure (00-005-0602), while the second one belongs to the aluminum sample holder [17,36]. A satisfying degree of crystallization might be inferred by the relatively high intensity and defined shape of the signals.

Figure **4** showed the XPS spectra of La(3d), Fe(2p) and O(1s) for the $LaFeO_3$ sample. The La(3d) spectra shows two doublets at around 836 and 853 eV corresponding to La($3d_{3/2}$) and La($3d_{5/2}$) orbitals, in particular, the energy gap between the peaks of the La($3d_{5/2}$) doublet is 3.8 eV, comparable with $La(OH)_3$ (3.9 ev) rather than La_2O_3 (4.6eV). Thus, it is possible

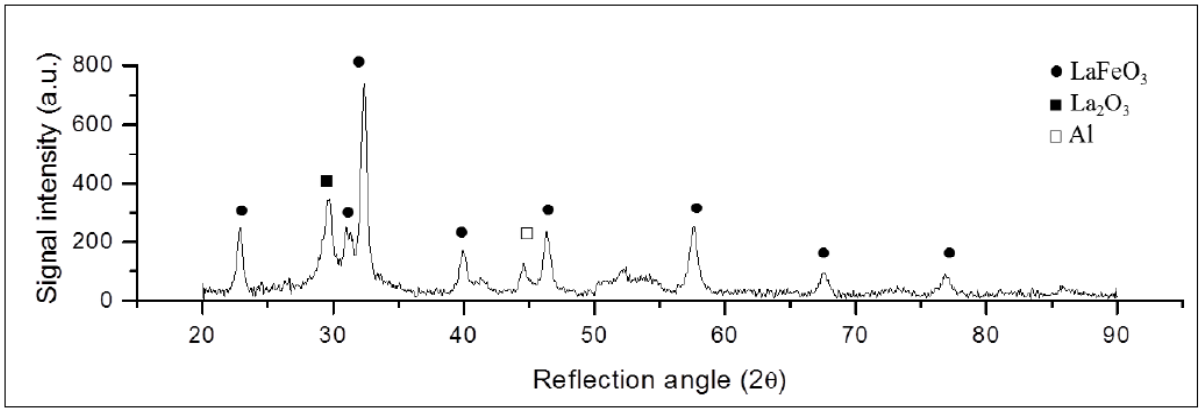

Figure 3: X-ray diffraction pattern (XRD) of the prepared $LaFeO_3$.

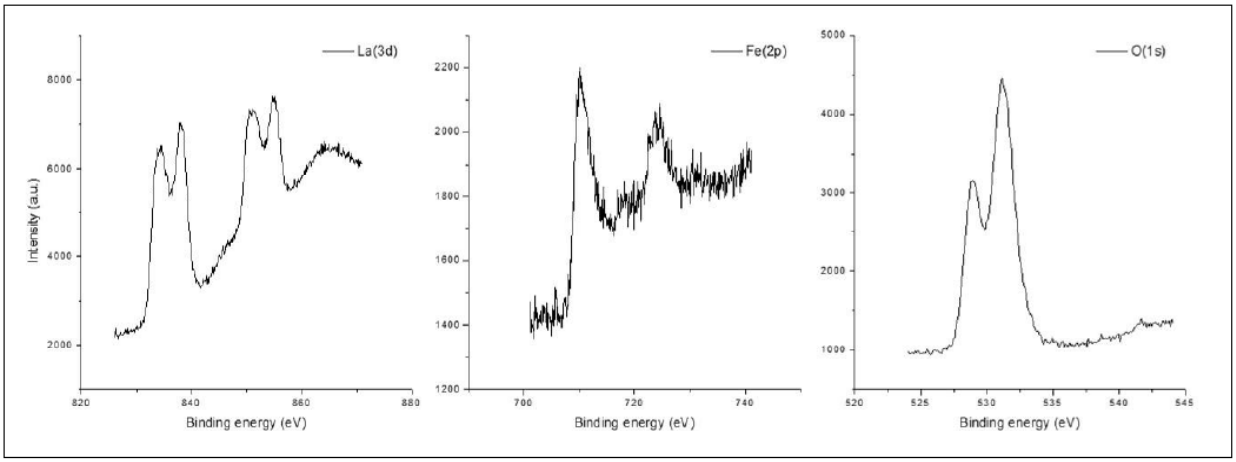

Figure 4: XPS spectra of $LaFeO_3$ with respect to La(3d), Fe(2p) and O(1s).

to infer that the surface is mostly composed by perovskite structures instead of La_2O_3, nevertheless, the XRD analysis clearly showed the presence of lanthanum oxide below the surface [37]. The XPS spectra of Fe(2p) shows two main signals related to $Fe(2p_{1/2})$ and $Fe(2p_{3/2})$ orbitals at 723.6 and 710.2 eV respectively, in agreement with the peaks obtained from Fe^{3+} oxides in similar materials [38]. After deconvolution, the O(1s) XPS signal can be divided in three peaks at 528.9, 531.1 and 532.2 eV, the peak at 528.9 can be attributed to lattice oxygen species, while the one at 531.1 and the hidden at 532.2 may be related to oxygen species such as HO^- and O^- chemisorbed on the surface. The presence of superficial adsorbed water is limited since the related signal at approximately 234 eV is negligible [39].

The reducibility of the catalyst expressed as consumed H_2 was investigated and reported in Figure **5**. The profile shows multiple peaks due to the presence of multiple iron oxides, in particular La-Fe-O and Fe-O, and also to an excess of oxygen with respect to the stoichiometric, as commonly observed in the materials obtained through combustion [40]. The principal peak at 500 °C is ascribed to the reduction of Fe^{3+} in the perovskite lattice, while the signals at 275 °C and 750 °C might be related to the presence of Fe_2O_3 moieties not observed in the XRD analysis. Previous studies showed that Fe_2O_3 reduction to Fe occurs in two steps involving the formation of Fe_3O_4 intermediates, giving rise to two H_2 consumption peak around 300 °C and 730 °C [41]. Moreover, the first peak could be overlapped with the reduction of the oxygen surplus from the lattice at low temperatures (200-300 °C).

In Figure **6** the FESEM images of the fresh catalyst (a, b) and of the used one (c) are reported. The grains

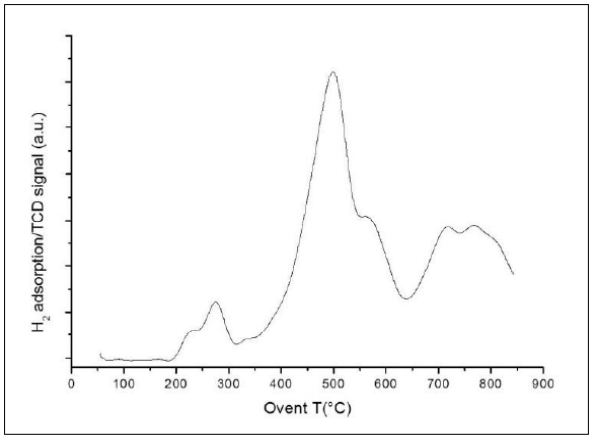

Figure 5: Temperature programmed reduction with H_2 (TPR-H_2) of $LaFeO_3$.

of $LaFeO_3$ are mainly present as nanospheres with an average diameter of 20 μm, which are arranged in larger stratified structures with different degree of agglomeration. Apparently, the used catalyst exhibits an increased average dimension of the spherical particles (40 μm), and occasionally, sodium salts and carbonaceous deposits were observed as consequence of the reaction environment.

3.2. Effect of the Reaction Temperature

The effect of the reactor temperature on the process performances was initially explored in the range 130-190 °C for reactions carried out at 10 bar of initial air pressure for 1h, without any catalyst or in the presence of $LaFeO_3$ (Figure **7**). In the case of the blank test, the AV conversion grows steadily from the 32.2% at 130 °C to 70.7% at 170 °C, while it seems to approach an asymptote at 190 °C with the 74.9%, the catalyzed test follows a similar behavior with conversion percentages lightly higher along all the temperatures profile by the 3% on the average. The vanillin yield slightly grows between 130 and 150 °C reaching the 7.5%, while the

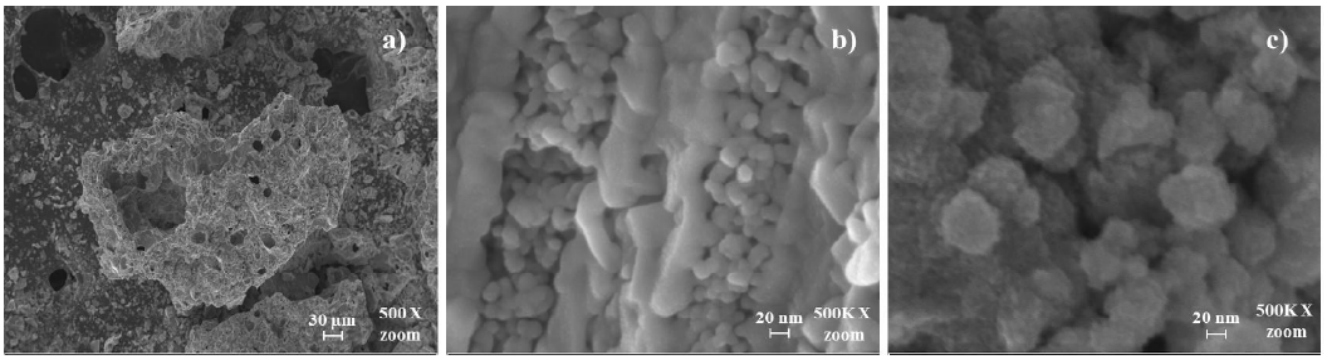

Figure 6: FESEM images of fresh $LaFeO_3$ fragments at 500 X (**a**) and 500K X (**b**) of magnification factor; a detail of the used catalyst follows (**c**).

temperature approach the 170 °C, vanillin starts growing significantly reaching the 16.2% and subsequently the 22.2% at 190°C. The highest selectivity towards vanillin was achieved as well at 190 °C with the 28.7% in the black setup, however, this result is lower than the expected. The performances offered by the perovskite in terms of vanillin productivity are better than the blank reaction in the temperatures range of 130-150 °C by 1-1.5%, furthermore, as the temperature increases the vanillin yield surprisingly decreases despite the enhanced AV conversion. This observation suggests that the catalyst provides higher oxidative strength causing higher AV conversion, but it also intensifies the degradation of vanillin to secondary products. This hypothesis is also reflected in Figure **8** where the process performances are reported as a function of temperature, and presented as carbon content of substrate (AV), main aromatic product (vanillin), and sum of the carboxylic acids measured in the aqueous fraction. In both catalytic and blank tests, as the reaction temperature rises and the AV conversion increases is possible to observe a progressive decrease in its carbon content in favor of vanillin and CAs ones, vanillin peaks at 190 °C reaching the 20.5%$_c$ and the 18.4%$_c$ respectively for the blank and for the catalytic test. At the same time, the CAs yield peaks at 150 °C in both cases showing the 26.2%$_c$ and 25.4%$_c$ respectively for the blank and for the catalytic test, despite that, the acids yields achieved were lower than expected due to over oxidation to CO_2 which occurs especially at high temperature. Unfortunately, it was not possible to effectively quantitate the CO_2 by means of chromatographic analysis of the exhausted gas mixture due to the adopted alkaline media which chemically absorbs it as carbonate ion. Despite that, the carbon balance of the quantified products and of the residual AV exhibits a progressive decrease as the reaction temperature rise.

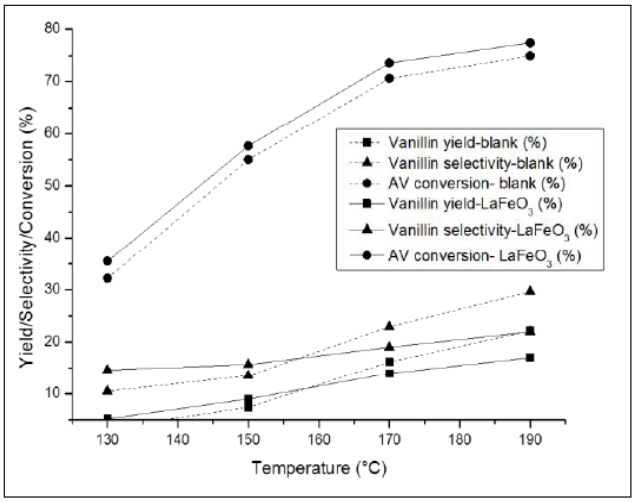

Figure 7: Performances comparison of the WAO of AV in the catalytic (normal line) and blank test (dotted line); acetovanillone conversion (●), vanillin yield (■) and vanillin selectivity (▲). Reaction conditions: 3.5 g/l of AV, 0.4 g of $LaFeO_3$ as catalyst, 25 ml of $NaOH_{aq}$ 2 M as solvent, 10 bar of air pressure, 1 h reaction time.

It is possible to consider this parameter as an index of the formation of CO_2, the higher the batch temperature, the higher the carbon lost from the quantitated balance. In fact, the carbon balance moved from the 89.1% achieved at 130 °C to 49.4% at 190 °C in the case of the black test, and similarly for the

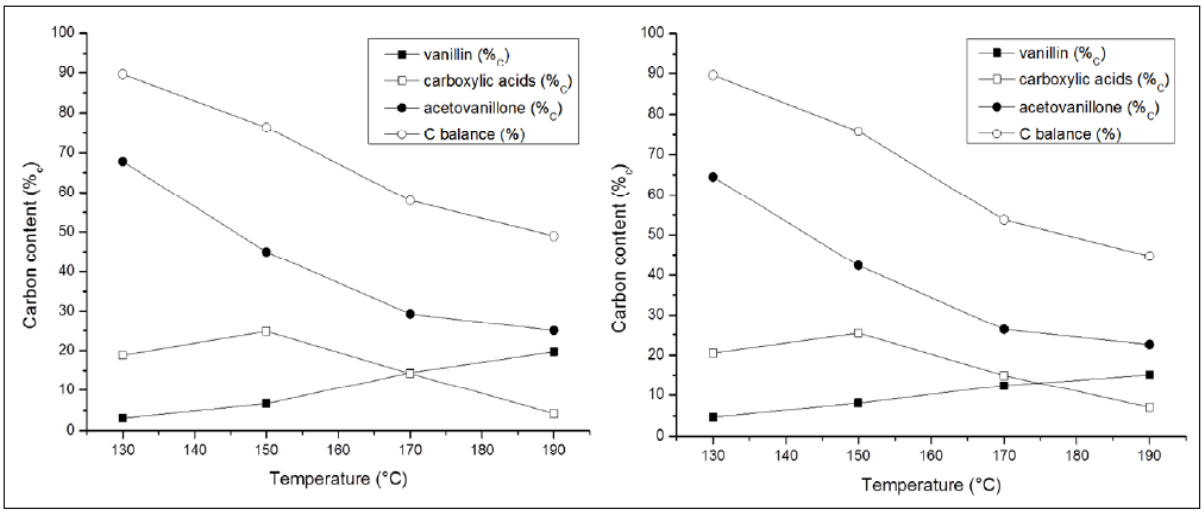

Figure 8: Performances comparison of the WAO of AV in the catalytic (right graph) and blank test (left graph); effect on carbon content distribution (%c) among acetovanillone (●), vanillin (■) and carboxylic acids (□), while the C balance (*) represents the sum of these contributions. Reaction conditions: 3.5 g/l of AV, 0.4 g of $LaFeO_3$ as catalyst, 25 ml of $NaOH_{aq}$ 2 M as solvent, 10 bar of air pressure, 1 h reaction time.

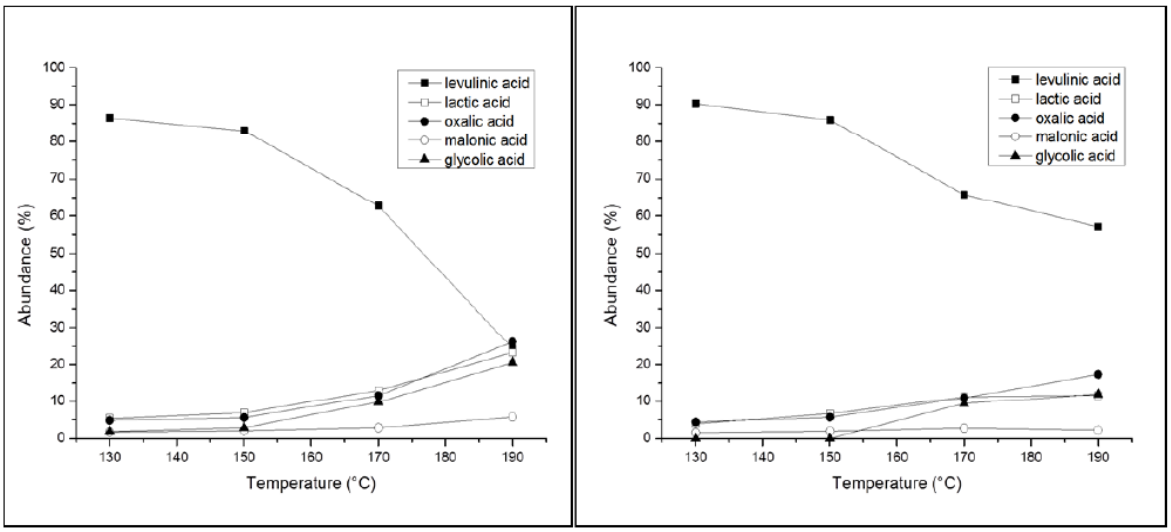

Figure 9: Effect of the presence of $LaFeO_3$ (right graph) on the carboxylic acids distribution (%) among levulinic acid(■), lactic acid (□), oxalic acid (●), malonic acid (○) and glycolic acid (▲) in comparison with the blank test (left graph). Reaction conditions: 3.5 g/l of AV, 0.4 g of $LaFeO_3$ as catalyst, 25 ml of $NaOH_{aq}$ 2 M as solvent, 1 h reaction time.

perovskite-catalyzed test it moved from the 87.4% obtained at 130°C to 48.5% at 190 °C.

The main products present in the residual aqueous phase after solvent extraction are shown in Figure **9** in the blank test levulinic acid represents the major compound with the 86.4% of abundance at 130 °C, and it dramatically decreases with the temperature, reaching a minimum of 24.4% at 190 °C. Other products, such as lactic, oxalic, malonic and glycolic acid increase progressively their abundances as the temperature increase, moving from 5.3%, 4.8%, 1.7%, and 1.8% at 130 °C up to 23.2%, 26.1%, 5.7% and 20.5% at 190 °C.

These observations suggest that the catalyst is capable to enhance the oxidative strength and AV conversion, in particular, it provides higher yield of vanillin when the temperature is below 150 °C compared with the blank test, however, as the reaction temperature rises, $LaFeO_3$ intensifies secondary oxidative reactions which causes the degradation of the aromatic ring of AV and vanillin to give CAs with consequent diminished vanillin selectivity.

3.3. Effect of the Oxidant Pressure

The effect of the change in the initial air pressure on the process performances was investigated in conditions of excess of oxidant in the range between 5 and 30 bar, with particular regard to AV conversion, vanillin yield and carboxylic acids yields. The experiments were carried out at 150 °C since is the temperature which offered the highest amount of quantified products with a maximum of 34%$_c$. On one hand, lower temperatures showed less conversion and fewer products, while on the other hand, higher temperatures enhanced over oxidation and consequently we observed the 30%$_c$ and the 25%$_c$ of products yield respectively at 170 and 190 °C in spite of the increased AV conversion.

In Figure **10** it is reported that AV conversion grows steadily with the increasing initial air pressure, rising from the 39% at 5 bar to 99% at 30 bar. At the same time, the vanillin yield slightly grows between 5 and 10 bar, when oxygen diffusion may be still a limiting factor,

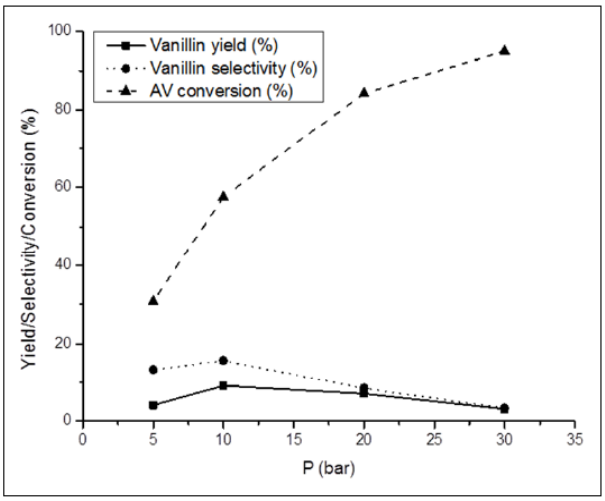

Figure 10: Effect of initial air pressure on acetovanillone conversion (dashed line), vanillin yield (normal line) and vanillin selectivity (dotted line). Reaction conditions: 3.5 g/l of AV, 0.4 g of $LaFeO_3$ as catalyst, 25 ml of $NaOH_{aq}$ 2 M as solvent, 1 h reaction time at 150 °C.

reaching a maximum yield of 9.1% with 15.7% of selectivity. Following, the increasing excess of oxidant leads vanillin yield and selectivity to decrease firmly, suggesting that its formation is challenging with secondary oxidative reactions.

In Figure **11** process performances are reported as a function of the initial air pressure and presented as carbon content of substrate (AV), main aromatic product (vanillin) and sum of the carboxylic acids measured in the aqueous fraction. As the oxidant pressure rises, the AV carbon content decreases steadily since the conversion rate had increased as previously observed, meanwhile, the vanillin carbon content initially rose to subsequently decrease with the growing oxidation rate to give carboxylic acids and CO_2. Accordingly, the yield in carboxylic acids progressively grows with the rise in the air pressure and the increasing AV conversion, however, the yields obtained are lower than expected due to over oxidation to CO_2.

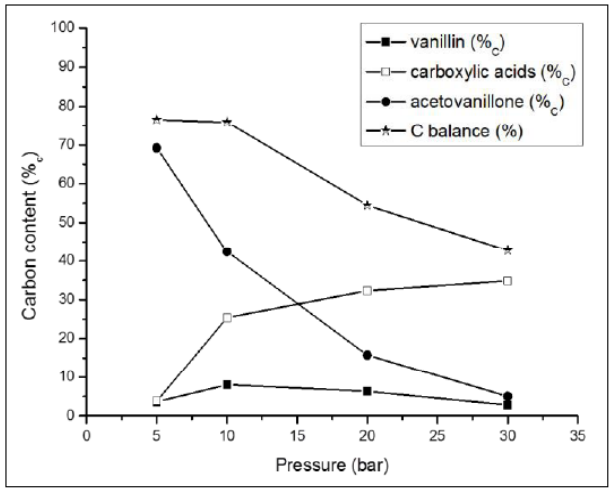

Figure 11: Effect of initial air pressure on carbon content distribution (%) among acetovanillone(●), vanillin (■) and carboxylic acids (□), while the C balance (*) represents the sum of these contributions. Reaction conditions: 3.5 g/l of AV, 0.4 g of $LaFeO_3$ as catalyst, 25 ml of $NaOH_{aq}$ 2 M as solvent, 1 h reaction time at 150 °C.

Unfortunately, it was not possible to effectively quantitate the CO_2 by means of chromatographic analysis of the exhausted gas mixture due to the adopted alkaline media which chemically absorbs it as carbonate ion. Despite that, the carbon balance of the quantified products and of the residual AV exhibits a progressive decrease as the initial air pressure increase. It is possible to consider this parameter as an index of the formation of CO_2, the larger the oxidant availability, the higher the carbon lost from the quantitated balance. In fact, the carbon balance moved from the 72% achieved with 5 bar of air to 45 % with 30 bar.

In Figure **12** it is shown that the CAs distribution dramatically changes moving from 5 bar of air load to 10 bar, while it lightly varies between 10 and 30 bar. In particular, oxalic and lactic acids represent the main compounds when the air pressure is 5 bar, but their abundances drop dramatically from 71.8% and 28.2% to 5.6% and 6.6% while increasing the reactor pressure to 10 bar. At the same time, the percentage of levulinic acid increases greatly from nearly zero to 85.5%, becoming the principal product. Moreover, the increase on the air pressure from 10 to 20, and 30 bar causes limited changes in the products distribution, with a linear trend which shows a gradual decrease in the levulinic acid percentage which reaches the 79.6% at 30 bar. Meanwhile, it was observed a slow increase of malonic and glycolic acids, which grow progressively from nearly zero to 4.3% and 3.9% respectively.

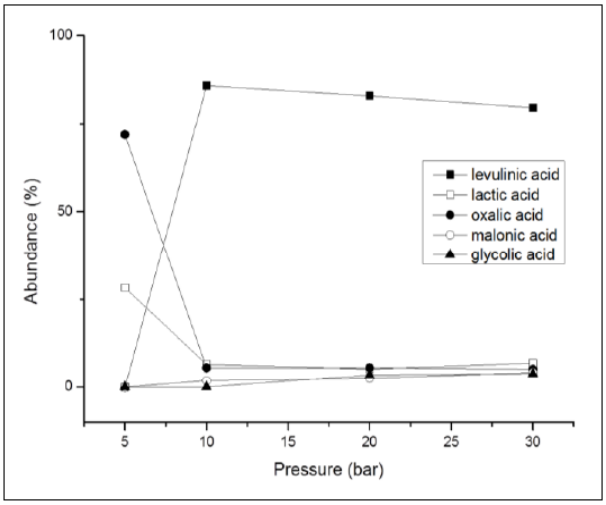

Figure 12: Effect of initial air pressure on the carboxylic acids distribution (%) among levulinic acid (■), lactic acid (□), oxalic acid (●), malonic acid (○) and glycolic acid (▲). Reaction conditions: 3.5 g/l of AV, 0.4 g of $LaFeO_3$ as catalyst, 25 ml of $NaOH_{aq}$ 2 M as solvent, 1 h reaction time at 150 °C.

3.4. Effect of the Variation of Temperature and Pressure

Afterwards, it was explored the effect of the reaction temperature on the process performances in the range 130-190 °C for two sets of experiments carried out at 10 and 20 bar of initial air pressure (Figure **13**). In both reaction sets the AV conversion grow firmly with the increasing batch temperature, in the case of 20 bar, it moves from 55% at 130 °C to 99.9% at 190 °C, while, in parallel, the AV conversion shift from 38% at 130 °C to 70% at 190°C in the case of 10 bar of air pressure.

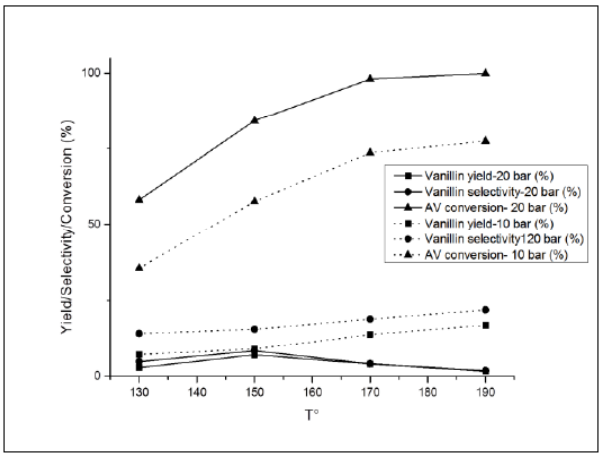

Figure 13: Effect of the reaction temperature on acetovanillone conversion (▲), vanillin yield (■) and vanillin selectivity (●). Reaction conditions: 3.5 g/l of AV, 0.4 g of $LaFeO_3$ as catalyst, 25 ml of $NaOH_{aq}$ 2 M as solvent, 1 h reaction time. The experiments were carried out at 10 bar (dotted line) and 20 bar (normal line) of air pressure.

Curiously, the vanillin productivity in terms of yield and selectivity does not follow the same trend in the two pressure sets. In the higher pressure experiment, vanillin exhibits an initial growth accordingly with the increasing substrate conversion, while at temperatures higher than 150°C it experiences a drop due to over oxidation reactions favored by the high temperature. In the lower pressure experiment, the initial vanillin yield is higher, as expected from the previous pressure investigations (Figure **13**), besides that, vanillin yield benefits from an higher reactor temperature reaching a maximum of 17% at 190° in contrast with the results of the 20 bar set. It is possible to infer that high pressure and high temperature negatively affect the selectivity of the oxidation towards vanillin by enhancing the oxidative strength and cracking reactions, however, a moderate air pressure close to 10 bar allows to achieve better performances and to exploit the kinetic advantages of a higher temperature while limiting the over oxidation.

In Figure **14** process performances of the 20 bar set are presented as a function of the batch temperature, as carbon content of substrate (AV), main aromatic product (vanillin), and sum of the carboxylic acids measured in the aqueous fraction. As the temperature rises, the AV conversion increases while its carbon content diminishes, vanillin carbon yield initially grows to subsequently decrease to secondary products, and the carbon content of the carboxylic acids slowly decreases to give CO_2. It worth noting that, the carbon balance steadily drops from the 80% at 130 °C to 30% at 190 °C, suggesting that the generation of CO_2 grows progressively with the increase in the batch temperature and it affects all the monitored compounds.

In Figure **15** it is shown how the CAs distribution changes moving from 130°C to 190°C for the two experiments sets carried out at 10 bar and 20 bar. In both cases, as the reaction temperature rises, we observed a general trend of progressive decrease of the higher molecular weight CAs, namely levulinic acid, in favor of lower molecular weight products. In the 10 bar set (left graph), the levulinic acid fraction falls from 90.3% to 57.1% while in the 20 bar set (right graph) the

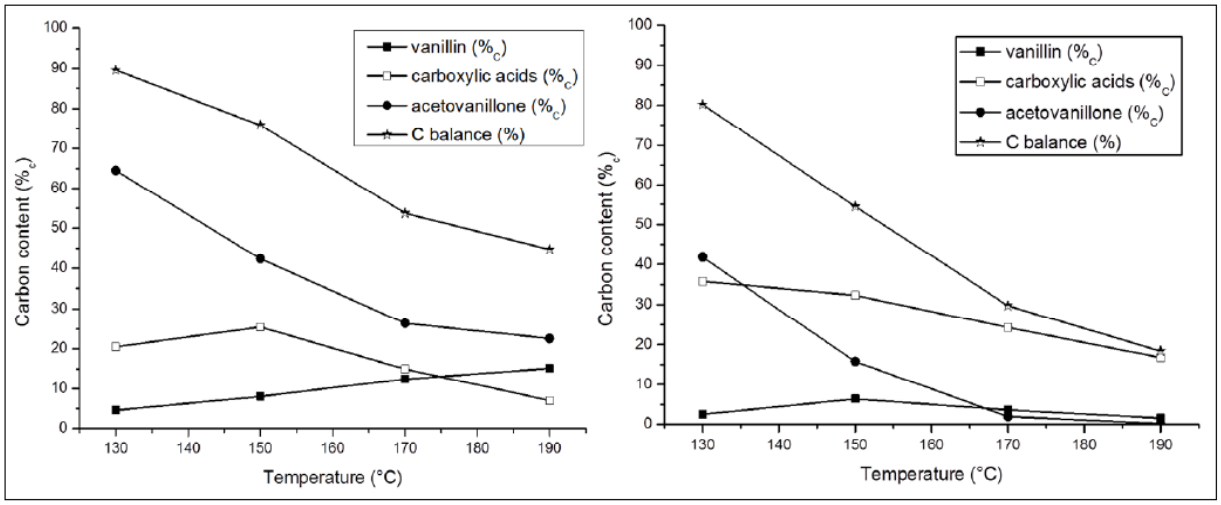

Figure 14: Effect of the reaction temperature on carbon content distribution (%) among acetovanillone(●), vanillin (■) and carboxylic acids (□), while the C balance (*) represents the sum of these contributions. Reaction conditions: 3.5 g/l of AV, 0.4 g of $LaFeO_3$ as catalyst, 25 ml of $NaOH_{aq}$ 2 M as solvent, 1 h reaction time for two sets of experiments carried out at 10 bar (left graph) and 20 bar (right graph).

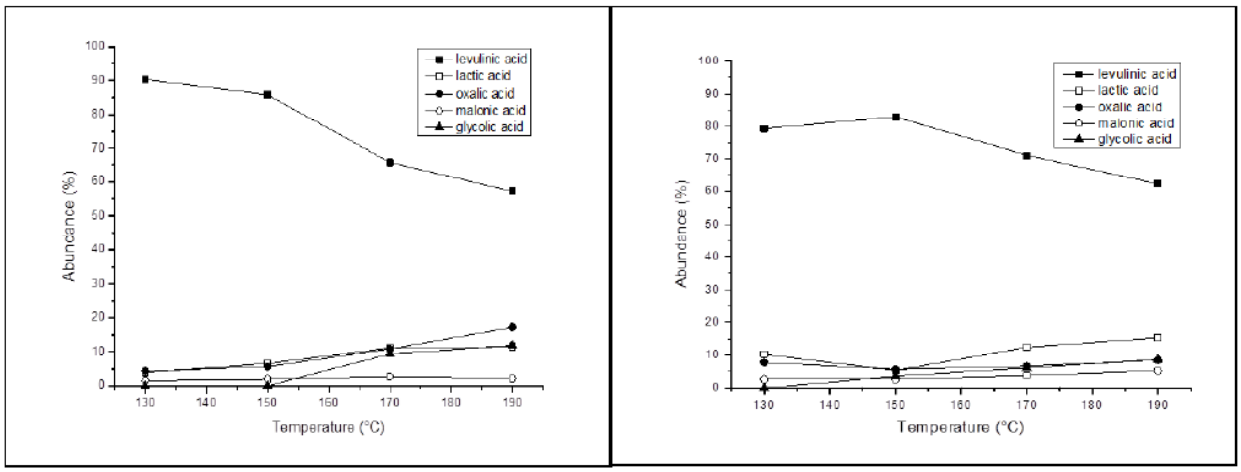

Figure 15: Effect of the reaction temperature on the carboxylic acids distribution (%) among levulinic acid(■), lactic acid (□), oxalic acid (●), malonic acid (○) and glycolic acid (▲) for two sets of test carried out at 10 bar (left graph) and 20 bar (right graph). Reaction conditions: 3.5 g/l of AV, 0.4 g of $LaFeO_3$ as catalyst, 25 ml of $NaOH_{aq}$ 2 M as solvent, 1 h reaction time.

percentage is only 79.4% at 130 °C, but curiously, it decreases only to 62.2% at 190 °C. Meanwhile, the relative abundance of the other quantified CAs generally grows; in the lower pressure set the second main product is oxalic acid which moves from 4.3% of abundance at 130 °C to reach the 17.3% at 190 °C, however, in the higher pressure set the second main CA is lactic acid which grows from 10.3% at 130 °C to 15.4% at 190 °C. In both cases, glycolic acid grows steadily with the increasing temperature moving from 0 to 11.9% in the 10 bar set and from 0 to 8.8% in the 20 bar set.

The presented data show that both temperature and air pressure significantly influence the reaction output, in this sense, a 3D visualization of the combined effects of these two parameters on the process performances may simplify and shorten data acquisition and interpretation (Figure **16**). In the a) section the 3D graph indicates that vanillin yield grows steadily with the temperature increase, showing a narrow maximum near the highest tested temperature, while the yield is close to zero around 130 °C. The increase of the air pressure has a beneficial effect at low reaction temperature by enhancing the substrate conversion and the vanillin yield to 8-9%, however, at higher reaction temperatures this effect is counterproductive due to the strengthened oxidative environment which promotes oxidative ring cleavage of the aromatic compounds. Similarly, in the b) section is reported the vanillin selectivity which differs from the previous graph in the low temperature section where, despite the decreased vanillin formation, the selectivity remains approximately stabile around 10%. Vanillin selectivity is still favored by high process temperature and limited air pressure, in fact high pressure values have the capability of dramatically reduce it in favor of CAs and CO_2. Lastly, in the c) section is shown the yield of CAs which, in contrast with the vanillin behavior, presents a broad flatter maximum due to the fact that this CAs yield comprises multiple products formed via multiple reaction pathways. It is possible to infer from the 3D visualization that the CAs formation is mostly favored by high air pres sures comprised between 25 and 30 bar, rather than the reaction temperature, since the maximum is comprised between 130 and 140 °C.

3.4. Insights on the Oxidative Mechanism

One of the oxidative mechanisms which have been proposed for the formation of carboxylic acids from lignin fragments, such as AV, involves the generation of highly active oxidative species in the presence of hydrogen peroxide, which brings to the formation of quinones intermediates. These compounds undergo further oxidation steps which lead to ring cleavage to give unsaturated carboxylic and bicarboxylic acids [29]. However, the results achieved suggest a totally different behavior, in the first instance quinone intermediates have never been observed in this study, nevertheless, these compounds might be highly unstable under the reaction conditions and they do not result among the products. The second observation is that the products distribution achieved among the carboxylic acids is not compatible with the above mentioned mechanism which involves the generation of unsaturated CAs, such as fumaric and maleic acids, generated from the cleavage of the aromatic ring. Other studies, on the alkaline oxidation of lignin moieties with hydrogen peroxide, hypothesize the

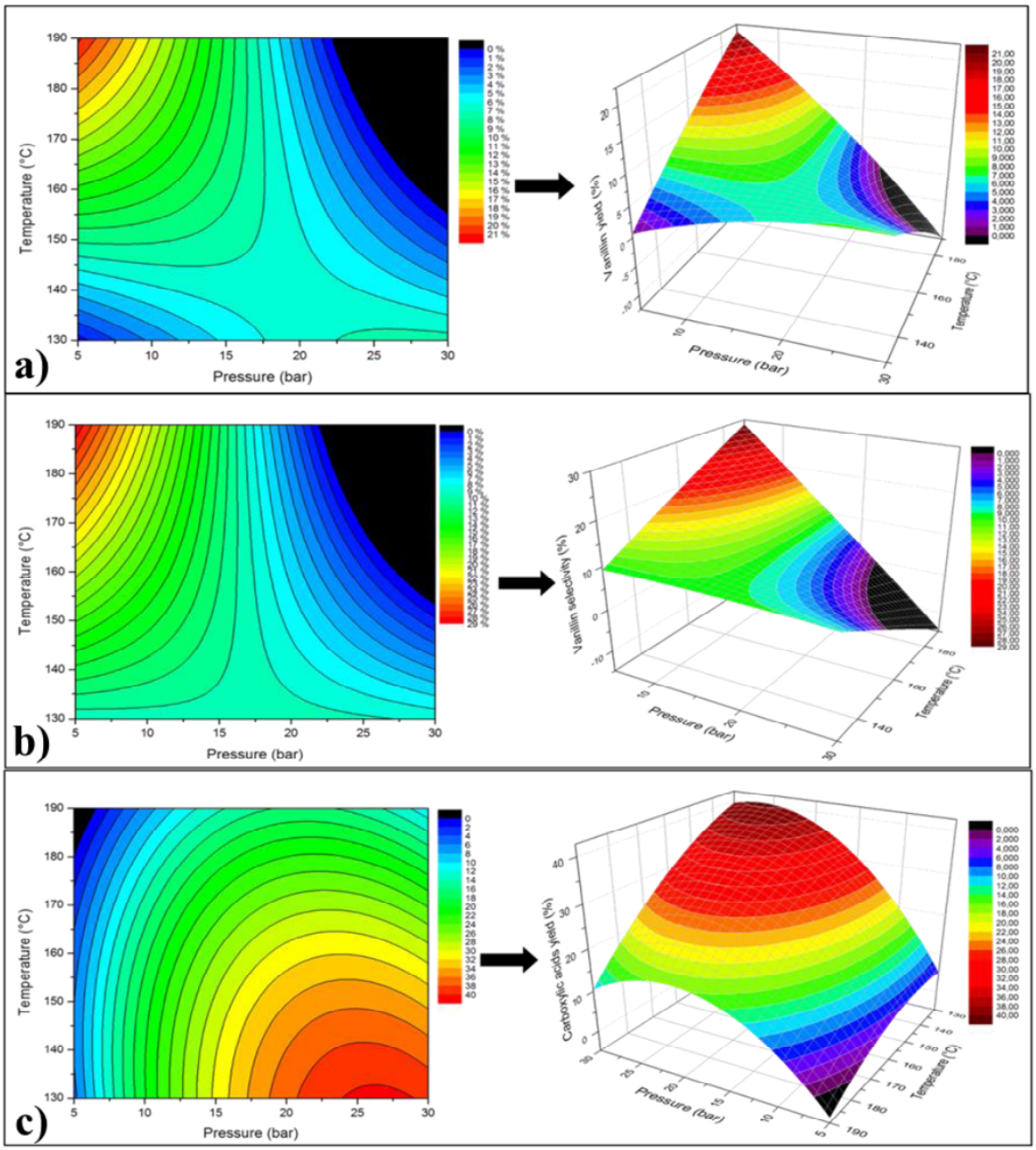

Figure 16: a. Vanillin yield (%) optimization; **b**. Vanillin selectivity (%) optimization; **c**. CAs carbon yield (%) optimization. 3D functions were obtained with Origin Pro 8.5 software and Poly 2D fitting optimization.

degradation of functionalized aromatics to low molecular weight CAs without chromophore intermediates such as quinones [28].

Herein, it is shown a more plausible reaction pathway for AV oxidation which take into consideration the oxidation of the ketone group to give vanillin as final product, and the competitive route which involves the phenolic group oxidation to give aromatic ring cleavage and the formation of low molecular weight CAs as we observed in our tests (Figure **17**) [20].

The alkaline environment allows the initial formation of the AV phenolate, which could undergo the oxidation of the ketonic methyl group (A) to give the corresponding alcohol and subsequently the aldehyde. Lastly, the interaction with the solvent causes the rearrangement of the ketone which ends with the elimination of H_2O and CO_2 to give the vanillin phenolate. Alternatively, the phenolate could experience electron rearrangement (B) with formation of radicals, which could interact with oxygen to give the oxidative opening of the aromatic ring, further

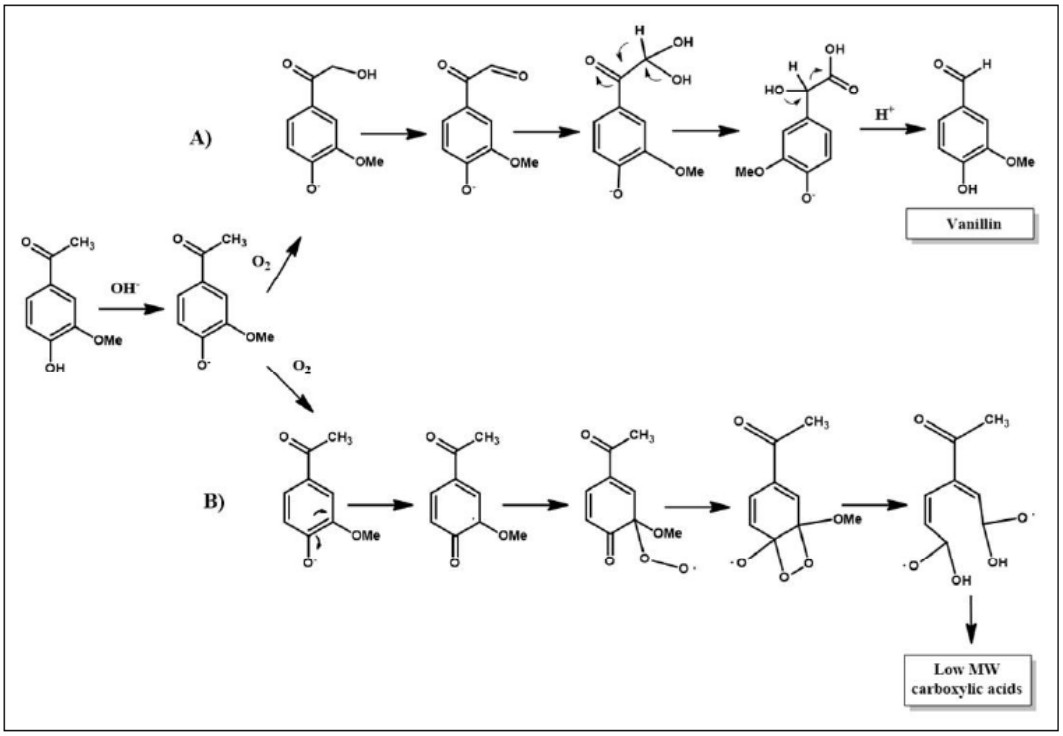

Figure 17: Plausible reaction mechanism for the generation of vanillin from acetovanillone, and competitive reaction of formation of carboxylic acids though aromatic ring opening.

rearrangements and oxidative cracking lead to the formation of lower molecular weight acid fragments. A previous work showed that the presence of radiation-induced ions is capable to induce the degradation of AV in water media [42]. This observation strengthens our hypothesis of a radicals-driven mechanism of AV degradation to CAs, but also, it helps to explain part of the carbon missed from the quantitation, since aromatic radicals can easily rearrange to form dimers of tricky detection.

4. CONCLUSIONS

The reaction behavior of acetovanillone (AV) as a model molecule for lignin during a WAO process was investigated. It was reported that, under the experimental conditions, vanillin is the principal aromatic product obtained from the oxidation of AV, while relevant amounts of CAs were observed as consequence of the aromatic ring cleavage. Main carboxylic compounds were oxalic, glycolic, lactic, malonic and levulinic acid.

A perovskite-type oxide, namely $LaFeO_3$, was synthetized, characterized, and used as catalyst in the reaction. The results suggest that process performances are mostly influenced by the reaction parameters rather than the presence of the catalyst, nevertheless, it enhances the oxidative strength in all the range of investigated temperatures. In particular, it favors the formation of vanillin at the lower temperature (130-150 °C), while at higher temperatures (170-190 °C) it decreases the vanillin yield in favor of CAs when compared with the blank test. It was shown that high temperatures (190 °C) rather than high oxidant pressures maximize the vanillin carbon yield to 22%, on the contrary the productivity of CAs is maximized at high oxidant pressures (30 bar) rather than high temperatures offering an overall carbon yield of 35%. Summarizing, the study proves the possible production of CAs from substituted aromatic using air as primary oxidant, and tries to clarify the mechanisms which drive the process.

REFERENCES

[1] Ragauskas AJ. The Path Forward for Biofuels and Biomaterials. Science (80-) 2006; 311: 484-9. http://dx.doi.org/10.1126/science.1114736

[2] Laskar DD, Yang B, Wang H, Lee J. Pathways for biomass-derived lignin to hydrocarbon fuels. Biofuels, Bioprod Biorefining 2013; 7: 602-26 http://dx.doi.org/10.1002/bbb.1422

[3] Ma R, Xu Y, Zhang X. Catalytic oxidation of biorefinery lignin to value-added chemicals to support sustainable biofuel production. ChemSusChem 2015; 8: 24-51. http://dx.doi.org/10.1002/cssc.201402503

[4] Sun Y, Cheng J. Hydrolysis of lignocellulosic materials for ethanol production : a review q. Bioresour Technol 2002; 83:

1-11.
http://dx.doi.org/10.1016/S0960-8524(01)00212-7

[5] Kawaguchi H, Hasunuma T, Ogino C, Kondo A. Bioprocessing of bio-based chemicals produced from lignocellulosic feedstocks. Curr Opin Biotechnol 2016; 42: 30-9.
http://dx.doi.org/10.1016/j.copbio.2016.02.031

[6] Isikgor FH, C. Remzi Becer. Lignocellulosic Biomass: a sustainable platform for production of bio-based chemicals and polymers. Polym Chem 2015; 6: 4497-559.
http://dx.doi.org/10.1039/c3py00085k

[7] Doherty WOS, Mousavioun P, Fellows CM. Value-adding to cellulosic ethanol: Lignin polymers. Ind Crops Prod 2011; 33: 259-76.
http://dx.doi.org/10.1016/j.indcrop.2010.10.022

[8] Heitner C, Dimmel D, Schmidt J. Lignin and Lignans: Advances in chemistry. CRC Press Taylor Fr Gr 2010; 683.
http://dx.doi.org/10.1016/0076-6879(88)61028-7

[9] Sánchez ÓJ, Cardona CA. Trends in biotechnological production of fuel ethanol from different feedstocks. Bioresour Technol 2008; 99: 5270-95.
http://dx.doi.org/10.1016/j.biortech.2007.11.013

[10] Holladay JE, White JF, Bozell JJ, Johnson D. Top Value-Added Chemicals from Biomass - Volume II:Results of Screening for Potential Candidates from Biorefinery Lignin. vol. II. Richland, WA: 2007.
http://dx.doi.org/10.2172/921839

[11] Gosselink RJA, De Jong E, Guran B, Abächerli A. Co-ordination network for lignin - Standardisation, production and applications adapted to market requirements (EUROLIGNIN). Ind Crops Prod 2004; 20: 121-9.
http://dx.doi.org/10.1016/j.indcrop.2004.04.015

[12] Zakzeski J, Bruijnincx PCA, Jongerius AL, Weckhuysen BM. The Catalytic Valorization of Ligning for the Production of Renewable Chemicals Chem Rev 2010; 110: 3552-99.
http://dx.doi.org/10.1021/cr900354u

[13] Lange H, Decina S, Crestini C. Oxidative upgrade of lignin - Recent routes reviewed. Eur Polym J 2013; 49: 1151-73.
http://dx.doi.org/10.1016/j.eurpolymj.2013.03.002

[14] Sales FG, Maranhão LCA, Lima Filho NM, Abreu CAM. Kinetic Evaluation and Modeling of Lignin Catalytic Wet Oxidation to Selective Production of Aromatic Aldehydes. Ind Eng Chem Res 2006; 45: 6627-31.
http://dx.doi.org/10.1021/ie0601697

[15] Partenheimer W. The aerobic oxidative cleavage of lignin to produce hydroxyaromatic benzaldehydes and carboxylic acids via metal/bromide catalysts in acetic acid/water mixtures. Adv Synth Catal 2009; 351: 456-66.
http://dx.doi.org/10.1002/adsc.200800614

[16] Villar JC, Caperos A, Garcia-Ochoa F. Oxidation of hardwood kraft-lignin to phenolic derivatives with oxygen as oxidant. Wood Sci Technol 2001; 35: 245-55.
http://dx.doi.org/10.1007/s002260100089

[17] Bernardi M, Deorsola FA, Fino D, Russo N. Catalytic Wet Air Oxidation of Maleic Acid Over Lanthanum-Based Perovskites Synthesized by Solution Combustion Synthesis. Waste and Biomass Valorization 2014; 5: 857-63.
http://dx.doi.org/10.1007/s12649-014-9301-z

[18] Das L, Kolar P, Sharma-Shivappa R. Heterogeneous catalytic oxidation of lignin into value-added chemicals. Biofuels 2012; 3: 155-66.
http://dx.doi.org/10.4155/bfs.12.5

[19] Zhang J, Deng H, Lin L. Wet aerobic oxidation of lignin into aromatic aldehydes catalysed by a perovskite-type oxide: LaFe1-xCuxO3 (x=0, 0.1, 0.2). Molecules 2009; 14: 2747-57.
http://dx.doi.org/10.3390/molecules14082747

[20] Alunga KR, Ye Y-Y, Li S-RL, Liu Y-Q. Catalytic oxidation of lignin-acetoderivatuves: a potential new recovery route for value-added aromatic aldehydes from acetoderivatives. Catal Sci Technol 2015; 5: 3746-53.
http://dx.doi.org/10.1039/C5CY00419E

[21] Gupta B, Revagade N, Hilborn J. Poly(lactic acid) fiber: An overview. Prog Polym Sci 2007; 32: 455-82.
http://dx.doi.org/10.1016/j.progpolymsci.2007.01.005

[22] Belitz H-D, Grosch W, Schieberle P. Food Chemistry. Berlin, Heidelberg: Springer Berlin Heidelberg; 2004.
http://dx.doi.org/10.1007/978-3-662-07279-0

[23] Lochab B, Shukla S, Varma IK. Naturally occurring phenolic sources: monomers and polymers. RSC Adv 2014; 4: 21712.
http://dx.doi.org/10.1039/c4ra00181h

[24] Fache M, Boutevin B, Caillol S. Vanillin Production from Lignin and Its Use as a Renewable Chemical. ACS Sustain Chem Eng 2016; 4: 35-46.
http://dx.doi.org/10.1021/acssuschemeng.5b01344

[25] Fache M, Boutevin B, Caillol S. Epoxy thermosets from model mixtures of the lignin-to-vanillin process. Green Chem 2016; 18: 712-25.
http://dx.doi.org/10.1039/C5GC01070E

[26] Stewart D. Lignin as a base material for materials applications: Chemistry, application and economics. Ind Crops Prod 2008;27:202-7.
http://dx.doi.org/10.1016/j.indcrop.2007.07.008

[27] Niemelä K, Alén R, Sjöström E. The Formation of Carboxylic Acids during Kraft and Kraft-Anthraquinone Pulping of Birch Wood. Holzforschung 1985; 39: 167-72.
http://dx.doi.org/10.1515/hfsg.1985.39.3.167

[28] Xiang Q, Lee YY. Oxidative cracking of precipitated hardwood lignin by hydrogen peroxide. Appl Biochem Biotechnol 2000; 84-86: 153-62.
http://dx.doi.org/10.1385/ABAB:84-86:1-9:153

[29] Ma R, Guo M, Zhang X. Selective conversion of biorefinery lignin into dicarboxylic acids. ChemSusChem 2014; 7: 412-5. doi:10.1002/cssc.201300964.
http://dx.doi.org/10.1002/cssc.201300964

[30] Wu G, Heitz M. Catalytic Mechanism of Cu 2+ and Fe 3+ in Alkaline O 2 Oxidation of Lignin. J Wood Chem Technol 1995; 15: 189-202.
http://dx.doi.org/10.1080/02773819508009507

[31] Zhu J, Chen J. Perovskites: Structure, Properties and Uses. New York: Nova Science Publishers, Inc; 2010.

[32] Toledano A, Serrano L, Labidi J. Improving base catalyzed lignin depolymerization by avoiding lignin repolymerization. Fuel 2014; 116: 617-24.
http://dx.doi.org/10.1016/j.fuel.2013.08.071

[33] Karhunen P, Rummakko P, Sipilä J, Brunow G, Kilpeläinen I. The formation of dibenzodioxocin structures by oxidative coupling. A model reaction for lignin biosynthesis. Tetrahedron Lett 1995; 36: 4501-4.
http://dx.doi.org/10.1016/0040-4039(95)00769-9

[34] Gellerstedt. Structural changes in lignin during oxygen bleaching. Paper dedicated to Prof. Karl Kratzl on the occasion of his 70th birthday. Nord Pulp Pap Res J 1986; 1: 014-7.
http://dx.doi.org/10.3183/NPPRJ-1986-01-03-p014-017

[35] Atta NF, Galal A, El-Ads EH. Perovskite Nanomaterials - Synthesis, Characterization, and Applications. Perovskite Mater. - Synth. Characterisation, Prop Appl InTech; 2016.
http://dx.doi.org/10.5772/61280

[36] Nakayama S. LaFeO3 perovskite-type oxide prepared by oxide-mixing, co-precipitation and complex synthesis methods. J Mater Sci 2001; 36: 5643-8.
http://dx.doi.org/10.1023/A:1012526018348

[37] Sunding MF, Hadidi K, Diplas S, Løvvik OM, Norby TE, Gunnæs AE. XPS characterisation of in situ treated lanthanum oxide and hydroxide using tailored charge referencing and peak fitting procedures. J Electron Spectros Relat Phenomena 2011; 184: 399-409.
http://dx.doi.org/10.1016/j.elspec.2011.04.002

[38] Biesinger MC, Payne BP, Grosvenor AP, Lau LWM, Gerson AR, Smart RSC. Resolving surface chemical states in XPS analysis of first row transition metals, oxides and hydroxides: Cr, Mn, Fe, Co and Ni. Appl Surf Sci 2011; 257: 2717-30. http://dx.doi.org/10.1016/j.apsusc.2010.10.051

[39] Cho Y-G, Choi K-H, Kim Y-R, Jung J-S, Lee S-H. Characterization and Catalytic Properties of Surface La-rich LaFeO 3 Perovskite. Bull Korean Chem Soc 2009; 30: 1368-72. http://dx.doi.org/10.5012/bkcs.2009.30.6.1368

[40] Tascón JMD, Fierro JLG, Tejuca LG. Physicochemical properties of LaFeO3. Kinetics of reduction and of oxygen adsorption. J Chem Soc Faraday Trans 1 Phys Chem Condens Phases 1985; 81: 2399. http://dx.doi.org/10.1039/f19858102399

[41] Varma S, Wani B., Gupta N. Redox behavior and catalytic activity of La-Fe-V-O mixed oxides. Appl Catal A Gen 2003; 241: 341-8. http://dx.doi.org/10.1016/S0926-860X(02)00492-1

[42] Gonter K, Takács E, Wojnárovits L. High-energy ionising radiation initiated decomposition of acetovanillone. Radiat Phys Chem 2012; 81: 1495-8. http://dx.doi.org/10.1016/j.radphyschem.2011.11.011

Received on 26-09-2016 Accepted on 18-10-2016 Published on 27-10-2016

http://dx.doi.org/10.15379/2408-9834.2016.03.02.02